UDC 544.52: 546.21 doi: 10.33609/0041-6045.85.11.2019.63-72

**V.S.Vorobets*, G.Ya.Kolbasov, S.Ya.Oblovatna, O.O.Salamakha, S.V.Karpenko, I.A.Rusetskyi**

# SYNTHESIS, PHOTO- AND ELECTROCATALYTIC PROPERTIES OF NANOSTRUCTURED Ce–$TiO_2$ FILMS

*V.I.Vernadsky Institute of General and Inorganic Chemistry of National Academy of Sciences of Ukraine, 32/34 Academic Palladin Avenue, Kyiv, 03142, Ukraine*
**e-mail: vorobetsvs@i.ua*

Electrocatalytic films based on nanodispersed titanium dioxide modified by Ce(III) were synthesized by sol-gel method and characterized by X-ray diffraction and ultraviolet-visible photocurrent spectra. The average size of nanoparticles was no more than 11 nm. The XRD results indicated that $TiO_2$ and Ce–$TiO_2$ electrodes with Ce concentrations up to 5 % calcined at 500°C consisted of anatase as the unique phase. The photocurrent spectra of the Ce–$TiO_2$ electrodes (0 ≤ Ce concentration ≤ 2% mol.) showed a stronger current in the UV range and a shift in the flat-band potential ($E_{fb}$) towards more negative values than that of $TiO_2$ electrodes. Electrocatalytic properties of $TiO_2$ and Ce–$TiO_2$ electrodes were investigated in the process of oxygen electroreduction. It has been found by *I–E* curves measurements that the potential of oxygen reduction changes with the film composition. Modifying of $TiO_2$ films by Ce(III) improves catalytic activity of Ce–$TiO_2$ electrodes ( Ce concentration up to 2% mol.) in the reaction of oxygen electroreduction, that appears in decreasing of oxygen reduction potential $E_{O2}$ and increasing of dynamic range of $O_2$ electroreduction potentials. The high electrocatalytic activity of Ce–$TiO_2$ electrodes in the oxygen reduction process may be due to the formation of catalytically active centers which activity may decrease in the presence of an amorphous phase. The correlation between photo- and electrocatalytic properties and structural changes occurring in Ce–$TiO_2$ films on increasing the cerium content is observed. The electrodes investigated were distinguished by a high sensitivity to dissolved oxygen ((4-5)·$10^{-6}$ g·$l^{-1}$) and high reproducibility of characteristics in long-time cycling. These electrodes promise much as reusable electrode materials in electrochemical sensors for the determination of oxygen in liquids.

K e y w o r d s: titanium dioxide, cerium, oxygen electroreduction, catalytic activity, photosensitivity.

*INTRODUCTION.*Titanium dioxide is a promising material for application in optical and protective coatings, electrochemical devices, as oxygen reduction catalyst environmental photocatalysis, for the generation of electricity in the solar cells, gas sensors,etc. The catalytic activity of titania increases greatly when rare earth dopednanoparticles are used [1]. In this paper we present study results of photo- and electrocatalytic properties of electrodes based on nanostructured titanium oxide films modified by Ce.

*EXPERIMENT AND DISCUSSION OF THE RESULTS.* Nanoscale titanium dioxide $TiO_2$ was synthesized by the sol-gel method from titanium(IV) tetraisopropoxide in the presence of the non-ionic surfactant Triton X-100 [1]. An appropriate amount of Triton X-100 was dissolved in ethanol (EtOH), after which acetic acid (AcOH) was added to the solution. Then a titanium dioxide precursor, titanium tetraisopropoxide (TTIP), was added to the solution with vigorous stirring. The molar ratio of the components was Triton X-100 : EtOH : AcOH : TTIP=0.5 : 69 : 6 : 1. To prepare $TiO_2$ modified with cerium ions, appropriate amounts of $CeCl_3$ were added into the precursor to reach the cerium content of 0.5, 1, 2, 3, 5, 8 and 10% mol. To fabricate $TiO_2$ and Ce-$TiO_2$ films, transparent sol was deposited on pre-prepared Ti substrates and annealed in air at 500 °C. Preliminary preparation of Ti substrate included degreasing with acetone or carbon tetrachloride, as well as chemical etching in a mixture of HF and $HNO_3$ acids for 3-5 minutes, which helps to remove the surface oxide layer from the titanium foil, and also provides better adhesion of $TiO_2$ sol with substrate. Sol was deposited on a conducting substrate by the immersion method. To this end, the first sol layer was deposited on a prepared substrate; after that, the electrode was dried in an SNOL 58/350 laboratory oven at 120 °C for 10 minutes. This procedure was repeated 10 times. The electrodes with deposited layers based on Ce–$TiO_2$ sol were annealed in air in an SNOL 7.2/900 muffle furnace at $t$=500°C for 30 min and cooled at room temperature.

The phase composition and crystal structure of the obtained samples were studied by means of a DRON-3M diffractometer (monochromatic Cu$K_\alpha$ radiation with nickel filter, $\lambda$=1.5418Å) at 30 kV, 20 mA in an angle range of 2$\theta$=10–90°. To identify the diffractograms, the JCPDS database was used. The diffractograms were processed using the computer programs X-Ray and Match. The size of crystallites (coherent-scattering regions) of the obtained samples was calculated from the Scherrer equation using the most intense (101) anatase diffraction peak.

The photosensitivity of the samples and their photoelectrochemical characteristics (spectral dependence of the photocurrent quantum yield and flat-band potential) were estimated from photocurrent values in wavelength range of 250–600 nm. The photoelectrochemical investigations were carried out in 1N KCl solution in a quartz electrochemical cell with separated cathode and anode spaces using an MDR-2 monochromator and a DKSSh 500 high-pressure xenon lamp. An Ag/AgCl electrode was used as a reference electrode, and a platinum electrode was used as an auxiliary electrode.

The electrocatalytic activity of electrodes based on $TiO_2$ and Ce-$TiO_2$ films during oxygen electroreduction and the possibility of using them in sensing system were studied under potentiodynamic conditions using a PC-based electrochemical setup, which had the following characteristics: measured currents $2\cdot10^{-9} \div 10^{-1}$ A, potential scan rate 0.01÷50 mV·$s^{-1}$, working electrode potential range -4 ÷ +4 V. $TiO_2$- and Ce-$TiO_2$ – based films deposited on a titanium substrate were used as a working electrode. The measurements were made in a 0.9% NaCl solution.

*Structure of powders*. X-ray patterns of powders obtained from the precursors of $TiO_2$ and Ce–$TiO_2$ films with a cerium content of 0.5-10 % mol. are shown in fig 1. In the X-ray patterns of both the initial $TiO_2$ and cerium-doped $TiO_2$ there are reflections typical of the crystalline anatase phase (JCPDS, no 21-1272). The diffraction peaks at 25,3°, 37,8°, 48,0°, 53,9°, 55,0° and 62,7° are identified as the (101), (104), (200), (105), (211) and (204) reflections of the crystalline anatase phase. The diffraction peaks corresponding to the crystalline cerium phase in Ce–$TiO_2$ samples are not observed (fig 1).

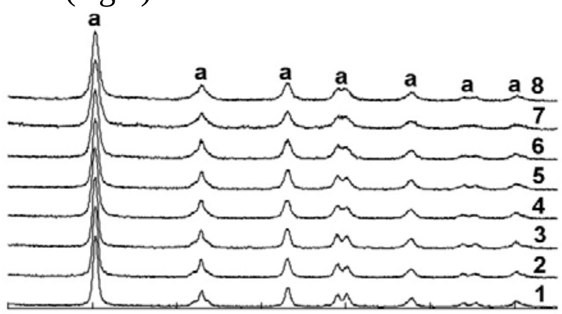


Fig 1. X-ray patterns of powders obtained at 500 ºC from precursors of films with a cerium content of (% mol.) : *1*–0; *2* –0,5; *3*–1; *4*–2; *5*–3; *6*–5; *7*–8; *8*–10.

As follows from Refs [2–8], cerium can be in the amorphous state [2], in the form of crystals of the cubic $CeO_2$ phase [3–5], but the incorporation of cerium ions into the anatase lattice is also possible [6]. It should be noted that the method used for making samples has a strong influence on the crystallization of mixed $TiO_2$ and Ce–$TiO_2$ oxides. When the sol-gel method is used, the cubic $CeO_2$ phase, besides anatase, crystallizes in the presence of surfactants at a higer molar Ce content (≥ 10 %mol.) [7, 8] and at a higher temperature than when using acids [2,4].

It can be seen that the anatase reflections become less intense with increasing Ce content при $2\theta > 55°$ (fig 1). According to the data of the authors of [2], who synthesized Ce–$TiO_2$ powders by the sol-gel method using Triton X-114 in cyclohexane without using an acid, this indicates that cerium in Ce–$TiO_2$ powders is probably present as an amorphous phase, and that the titanium dioxide crystallite size depends on the Ce content.

The broadening of diffraction peaks indicates that the obtained powders are nanocrystalline. The mean crystallite size was determined by the broadening of the most intense (101) peak from the Scherrer equation:

$$d = \frac{k\lambda}{\beta\cos\theta},$$

where $d$ is the mean crystallite size, $k$ is a constant ($k$ = 0.9), β is peak half-width, λ and θ are X-ray wavelength and reflection agle respectively. The (101) diffraction peak half-width was determined as the half-width of the Lorentzian fitting function, which de scribes the peak profile. The description of the profile of this diffraction peak by the Gaussian function was less satisfactory. The particle sizes calculated by the above procedure for $TiO_2$ and Ce–$TiO_2$ samples with a Ce content of o.5, 1, 2, 3, 5 %mol. are listed in table 1. The effect of the Ce content on the crystallite size D of anatase $TiO_2$ is given in table 1.

As follows from table 1, when the

T a b l e 1.
**Structural properties of investigated materials determined by using XRD**

| Composition | 2θ,º | *D, Å* | Lattice parameters | | |
|---|---|---|---|---|---|
| | | | *a*(Å) | *c*(Å) | *V*($Å^3$) |
| $TiO_2$ | 25,35 | 108.1 | 3.7826 | 9.5057 | 136.01 |
| 0.5%Ce/$TiO_2$ | 25,33 | 97.8 | 3.7831 | 9.5175 | 136.21 |
| 1%Ce/$TiO_2$ | 25,31 | 97.2 | 3.7854 | 9.5236 | 136.46 |
| 2%Ce/$TiO_2$ | 25,30 | 82.6 | 3.7861 | 9.5230 | 136.50 |
| 3%Ce/$TiO_2$ | 25,33 | 84.7 | 3.7848 | 9.5271 | 136.47 |
| 5%Ce/$TiO_2$ | 25,34 | 72.6 | 3.7818 | 9.5372 | 136.40 |

Ce content of modified samples is increased, the particle size decreases, which may be due to the presence of Ce–O–$TiO_2$ bonds, which impede the growth of crystalline grains [3,4].

The X-ray spectra of samples with a Ce content of 8 and 10 % mol. exhibit a weak broad peak at 2θ = 70º (fig 1, curves *7*, *8*), which corresponds to the presence of very small (~ 1 nm) $CeO_2$ crystallites, which agrees with the data of [2,5]. In spite of the fact that in the samples with high Ce content (8 and 10% mol.), cerium is in an amorphous phase, as was shown above, cubic $CeO_2$ crystallites can nucleate in the bulk of $TiO_2$ anatase [5]. However, they are difficult to detect by XRD because of very small size, which is below the limit of detection by XRD.

The X-ray patterns of Ce–$TiO_2$ samples with a Ce content of up to 2 %mol. , annealed at 500 $^0$C (fig 1) exhibited a broadening of typical anatase peaks and their shift to smaller angles (table 1, fig 2).

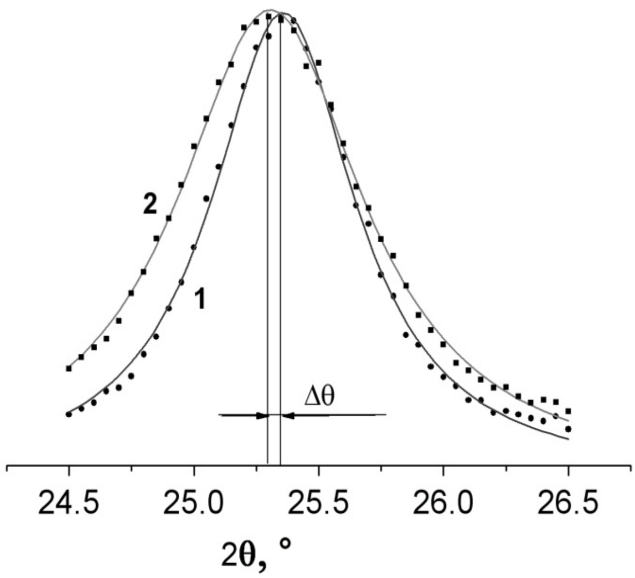


Fig 2. Decomposition of the (101) peak by means of the Lorentz function in X-ray patterns of films: *1* – $TiO_2$; *2* – 2%Ce–$TiO_2$.

This indicates that cerium ions are incorporated into the anatase lattice [6], though the difference in ionic radius between titanium ($Ti^{4+}$ = 0.68 Å) and cerium ($Ce^{4+}$ = 0.92 Å) is large. The values of the lattice parameters a and c as well as lattice volume V, calculated with the aid of the program X-Ray, increase with increasing the cerium content of samples to 2% (table 1), which also indicates the possibility of $Ce^{4+}$ ion incorporation into the anatase lattice. The obtained data agree with the data of the authors of [6], who showed that in spite of the large difference in ionic radius, Ce ions can replace $Ti^{4+}$ ions in the anatase lattice to form (≡ Ti–O–Ce–O–Ti≡) bonds. In this case, all $TiO_2$ can be saturated with a relatively small amount of Ce (because of the large difference between the radii of $Ti^{4+}$ and $Ce^{4+}$ ions); the rest of Ce is probably present on the surface as $CeO_2$. The authors of [6] also observed an expansion of the anatase unit cell for Ce-doped samples compared with pure $TiO_2$, which is an evidence of possible replacement of $Ti^{4+}$ in the anatase lattice by $Ce^{4+}$ ions.

In our case, increasing the Ce content (from 0,5 to 2 % mol.) in $TiO_2$ also led to an expansion of anatase lattice volume (table 1, fig 3). The increase in anatase lattice volume for the samples with a Ce content of up to 2 % mol. corresponds to the fact that $Ce^{4+}$ ions are incorporated into the anatase lattice. At a Ce content of about 2% mol., the $TiO_2$ lattice is already saturated with $Ce^{4+}$ ions, and $CeO_2$ is formed as an amorphous phase or very small nuclei, which agrees with the data of the authors of [4].

*Photoelectrochemical properties of Ce-$TiO_2$ films*. It has been found that the investigated electrodes based on Ce-$TiO_2$ films (table 2, samples 1–6) were photosensitive in a wavelength range of 250–400 nm, and that the quantum yield η depended largely upon the Ce content (table 2, fig 3) and was a maximum for 1% Ce–$TiO_2$ films.

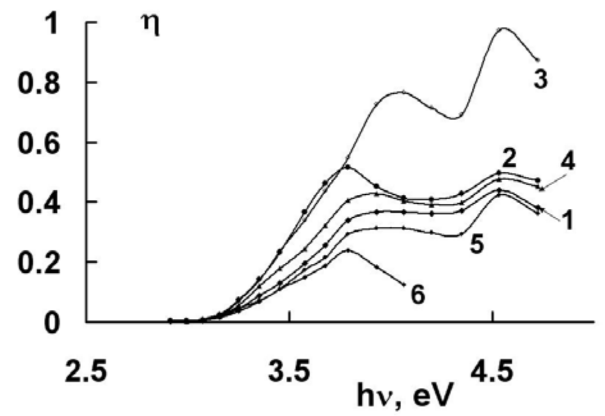


Fig.3. The spectral dependences of photocurrent quantum yield for $TiO_2$ and Ce–$TiO_2$ films with cerium content, % mol.: *1*–0; *2*–0.5; *3*–1; *4*–2; *5*–3; *6*–5.

The flat-band potential $E_{fb}$ and band gap energy $E_g$ for indirect photo-transitions in the forbidden band of $TiO_2$ have been determined from the photoelectrochemical current quantum yield spectra of electrodes based on obtained $TiO_2$ and Ce–$TiO_2$ films (table 2). The value of the flat-band potential $E_{fb}$ was determined from plots of photocurrent I vs potential E by extrapolating the linear portions of these plots to intersection with the abscissa axis [9]. The value of $E_{fb}$ allows one to estimate the change in the position of the conduction-band bottom of the obtained electrodes and the energy of electrons involved in reduction processes, including the oxygen electroreduction process [9]. To determine the band gap energy $E_g$, the photoelectrochemical current quantum yield spectra were reconstructed in the (hv

T a b l e 2

**Photoelectrochemical (η, $E_g$ and $E_{fb}$) and electrocatalytic ($E_{1/2}$ and $\Delta E$) properties of Ce–$TiO_2$ electrodes depending on cerium content**

| № | Composition | Photocurrent quantum yield η, a.u. | Band gap $E_g$,eV | Flat band potential $E_{fb}$, V | Oxygen half-wave potential $E_{1/2}$, V | Oxygen reduction range $\Delta E$,V |
|---|---|---|---|---|---|---|
| 1 | $TiO_2$ | 0.37 | 3.0 | -0.30 | -0.70 | 0,10 |
| 2 | 0.5%Ce/$TiO_2$ | 0.52 | 3.0 | -0.32 | -0.62 | 0,18 |
| 3 | 1%Ce/$TiO_2$ | 0.76 | 3.0 | -0.35 | -0.55 | 0,24 |
| 4 | 2%Ce/$TiO_2$ | 0.43 | 3.0 | -0.30 | -0.60 | 0,20 |
| 5 | 3%Ce/$TiO_2$ | 0.31 | 3.0 | -0.28 | -0.63 | 0,20 |
| 6 | 5%Ce/$TiO_2$ | 0.24 | 3.0 | -0.25 | -0.65 | 0,16 |

$\eta)^{0.5}$~hv coordinates for indirect allowed transitions in $TiO_2$, where η is quantum yield, and hv is quantum energy of light [9].

The value of quantum yield (η) for $TiO_2$ and Ce–$TiO_2$ samples was 0.24–0.76 (table 2). It should be noted that for the samples with Ce content of 0.5, 1 and 2% mol. , a significant increase in their photosensitivity relative to unmodified $TiO_2$, which manifests itself by an increase in the quantum yield of photoelectrochemical current, η (table 2, samples 2– 4), and a shift of the spectra to the long-wavelenth region (fig 3, curves *2– 4*) are observed. For the films with a Ce content of >2%, the values of the quantum yield of photocurrent were smaller compared with unmodified $TiO_2$ films (table2, fig 3, curves *5*, *6*). In this case, the band gap energy $E_g$ of the investigated electrodes did not change greatly (table 2). Taking this into consideration, we can consider that modification with Ce ions leads to the formation of photoactive defects in the forbidden band of $TiO_2$, whose activity may decrease with the formation of an amorphous phase (fig 3, curves *3*, *5*). The explanation of why the value of $E_g$ does not change at different contents of Ce lies in its usually much lower sensitivity with respect to progressing structural changes [2].

*Electrocatalytic properties of films*. The electrocatalytic properties of the obtained films of cerium-modified titanium were studied during oxygen electroreduction. This process is the basis of the operation of electrochemical $O_2$ sensors, which are designed for the determination of oxygen concentration in liquid media [8].

The polarization curves for electrodes based on Ce–$TiO_2$ films in physiologic solution 0.9%NaCl (pH 6.8) exhibited one polarographic wave of current at potentials of -0.5 to -1.0 V (vs silver-chloride electrode) with limiting current corresponding to oxygen reduction current (fig 4). At potentials of $E$< - 1.0 V, a hydrogen evolution reaction proceeded at the electrodes.

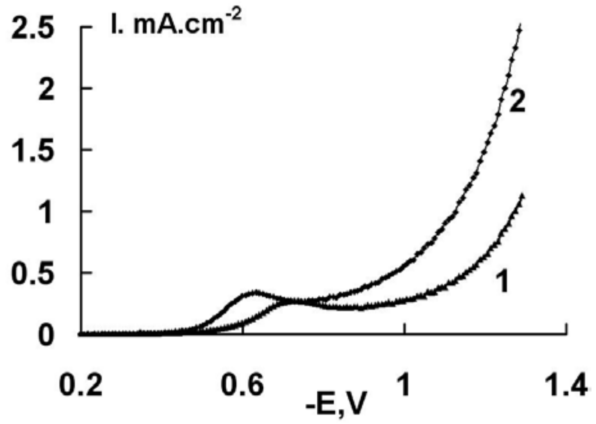


Fig 4. Polarization curves of oxygen electroreduction on Ce–$TiO_2$ electrodes: *1* – 5%Ce–$TiO_2$; *2* – 1%Ce–$TiO_2$. Potential scan rate 10 $mV{\cdot}s^{-1}$. Potentials are given relative to Ag/AgCl reference electrode.

Important characteristics of electrodes for the analysis of dissolved oxygen concentration are oxygen reduction potential or oxygen reduction half-wave potential $E_{1/2}$ on the cathodic polarization curve and the width of "electrochemical window", $\Delta E$ (dynamic potential range in which the oxygen content of the solution can be analyzed). The value of $E_{1/2}$ should be minimal to eliminate possible electrochemical side reactions, and the value of $\Delta E$ should be maximal to achieve high electrode sensitivity and measurement accuracy. From fig 4 it follows that in physiologic NaCl solution (pH 6.8), the value of $E_{1/2}$ at the electrodes with cerium content of 1% is – 0.55 V and is minimal among the obtained Ce–$TiO_2$ electrodes. The dynamic potential range of $O_2$ reduction on these electrodes was 0.24 V. The values of $E_{1/2}$ and $\Delta E$ for other electrodes are listed in table 2.

From table 2 it follows that modification of $TiO_2$ films with cerium increases the catalytic activity of electrodes based on them in the oxygen electroreduction reaction compared with unmodified $TiO_2$, which manifests itself by a decrease in oxygen reduction half-wave potential and an increase in the dynamic range of $O_2$ electroreduction. The electrodes with cerium content of 1% ($E_{1/2}$ = -0.55V, $\Delta E$ = 0.24V) showed the maximum electrocatalytic activity. At higher cerium content of films (>2%), the electrocatalytic activity of electrodes decreased (table 2). For samples with 5% cerium content, the values of $E_{1/2}$ = -0.65V, $\Delta E$ = 0.16V were obtained. The values of stationary potentials for samples with 1% and 5% cerium content are equal respectively to 0.17 V and 0.2 V. The decrease in catalytic activity with increasing cerium content may be due to, as in the case of photosensitivity, to the formation of catalytically active centers (crystalline defects), whose activity decreases during the formation of amorphous phase.

With repeated cycling of the potential, the polarization characteristics of the Ce – $TiO_2$ electrodes remained almost unchanged after the 3rd cycle, which indicates the high stability of the obtained electrodes and the possibility of using them to determine the concentration of dissolved oxygen.

Thus, electrodes based on Ce–$TiO_2$ films are distinguished by high electrocatalytic activity and stability in the process of oxygen reduction and are promising for use in electrochemical oxygen sensors.

The variation of the electrocatalytic ($E_{1/2}$) and photoelectrochemical (η and $E_{fb}$) properties of the $Ce–TiO_2$ films studied in this work as a function of cerium content is shown in fig 5.

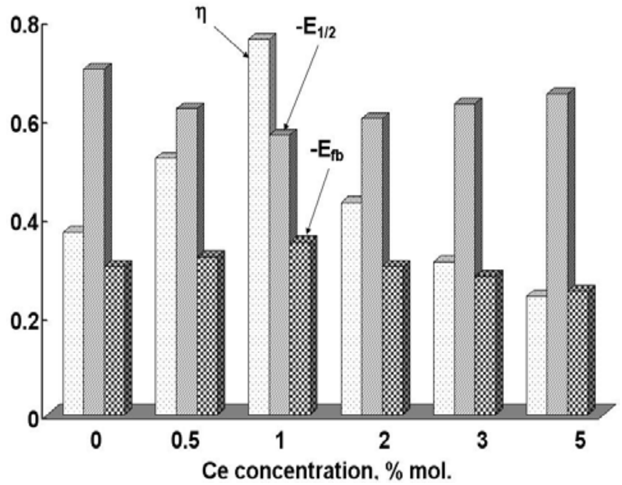


Fig 5. Dependence of the electrocatalytic ($E_{1/2}$) and photoelectrochemical (η and $E_{fb}$) properties of $Ce–TiO_2$ films on cerium content.

Thus, a correlation between photo- and electrocatalytic properties and structural changes occurring in $Ce-TiO_2$ films on increasing the cerium content is observed.

*CONCLUSION*. Powders and films of $TiO_2$ modified with Ce ions have been synthesized by sol-gel method. The $Ce–TiO_2$ powders with cerium content of 0.5–10% % mol. ($t_{annealing}$ = 500 °C) had an anatase crystal structure with a crystallite size of up to 11nm.

Electrodes based on $Ce–TiO_2$ films were photosensitive in a wavelength range of 250–400 nm. For samples with Ce content of 0.5, 1 and 2 % mol., an increase in the values of photocurrent quantum yield and a shift of spectra to the long-wavelength region compared with unmodified $TiO_2$ were observed. The subsequent increase of the cerium content led to a decrease in the photoactivity of samples.

The $Ce–TiO_2$ films were distinguished by an increased catalytic activity in the process of oxygen electroreduction, which manifested itself by a decrease in oxygen reduction half-wave potential and an increase in the dynamic range of $O_2$ electroreduction compared with unmodified titanium dioxide films. An increase in electrocatalytic activity was observed for cerium ion concentrations of up to 1%; the subsequent increase of the dopant content led to decrease in the activity of samples probably because of the formation of an amorphous phase. $Ce–TiO_2$ electrodes showed high stability and reproducibility of characteristics in the process of $O_2$ electroreduction. Synthesized electrode materials are most promising for use in electrochemical sensors for the determination of $O_2$ in liquid media.

СИНТЕЗ, ФОТО- ТА ЕЛЕКТРОКАТАЛІТИЧНІ ВЛАСТИВОСТІ НАНОСТРУКТУРОВАНИХ ПЛІВОК $Ce–TiO_2$

В.С. Воробець*, Г.Я. Колбасов, С.Я. Обловатна, О.О. Саламаха, С.В. Карпенко, І.А. Русецький

*Інститут загальної та неорганічної хімії ім. В.І. Вернадського НАН України, просп. Академіка Палладіна, 32/34, Київ, 03142, Україна*
**e-mail:vorobetsvs@i.ua*

Електрокаталітичні плівки на основі нанодисперсного діоксиду титану, модифікованого Ce(III), синтезовані золь-гель методом і охарактеризовані методами рентгенівської дифракції (XRD) та спектроскопії фотоелектрохімічного струму. Середній розмір наночастинок не перевищу-вав 11 нм. Результати XRD показали, що $TiO_2$ і Ce–$TiO_2$ порошки з концентраціями Ce до 5%, прожарені при 500 °C, мали кристалічну структуру анатазу. На спектрах фотоструму Ce–$TiO_2$ електродів (концентрація 0 ≤ Ce ≤ 2% мол.) спостерігався більш сильний струм в УФ-діапазоні і зсув потенціалу плоских зон ($E_{fb}$) до більш нега-тивних значень, у порівнянні з $TiO_2$ – електродами. Електрокаталітичні властивості електродів $TiO_2$ і Ce–$TiO_2$ досліджувалися в процесі електровідновлення кисню. За допомогою *I–E*-кривих було виявлено, що потенціал електровідновлення кисню залежав від складу плівок. Модифікування плівок TiO2 за допомогою Ce (III) покращує каталітичну активність електродів Ce–$TiO_2$ (концентрація Ce до 2 %мол.) у реакції електровідновлення кисню, що проявляється у зменшенні потенціалу відновлення кисню $E_{O_2}$ і збільшенні динамічного діапазону потенціалів електровідновлення $O_2$. Висока електрокаталітична активність електродів Ce–$TiO_2$ у процесі відновлення кисню , ймовірно, може бути обумовлена утворенням каталітично активних центрів, активність яких може зменшуватися в присутності аморфної фази. Спостерігається взаємозв'язок між фото- та електрокаталітичними властивостями та структурними змінами, що відбуваються в плівках Ce–$TiO_2$ при збільшенні вмісту церію. Досліджувані електроди відрізнялися високою чутливістю до розчиненого кисню (4–5)·10-6 г•$л^{-1}$) і високою відтворюваністю характеристик при тривалому циклюванні. Синтезовані електродні матеріали можуть бути використані в електрохімічних сенсорах для визначення $O_2$ у рідких середовищах.

К л ю ч о в і с л о в а: діоксид титану, церій, електровідновлення кисню, каталітична активність, фоточутливість.

## СИНТЕЗ, ФОТО- И ЭЛЕКТРОКАТАЛИТИЧЕСКИЕ СВОЙСТВА НАНОСТРУКТУРИРОВАННЫХ ПЛЕНОК Ce–$TiO_2$

В.С. Воробец*, Г.Я. Колбасов, С.Я. Обловатная, О.О. Саламаха, С.В. Карпенко, И.А. Русецкий

*Институт общей и неорганической химии им. В.И. Вернадского НАН Украины, просп. Академика Палладина, 32/34, Киев, 03142, Украина*
** e-mail:vorobetsvs@i.ua*

Электрокаталитические пленки на основе нанодисперсного диоксида титана, модифицированного Ce(III), синтезированы золь-гель методом и охарактеризованы методами рентгеновской дифракции (XRD) и спектроскопии фотоэлектрохимического тока. Результаты XRD показали, что $TiO_2$ и Ce–$TiO_2$ порошки с концентрациями Ce до 5%, отожженные при 500 °C, имели кристаллическую структуру анатаза. На спектрах фототока Ce–$TiO_2$ электродов (концентрация 0 ≤ Ce ≤ 2 % мол.) наблюдался более сильный ток в УФ-диапазоне и смещение потенциала плоских зон ($E_{fb}$) в сторону более отрицательных значений, по сравнению с $TiO_2$-электродами. Повышение электокаталитической активности Ce-$TiO_2$ электродов в процессе электровосстановления кислорода по сравнению с немодифицированным $TiO_2$ наблюдается для пленок с концентрациями Ce до 5%. Синтезированные пленки могут быть использованы в электрохимических сенсорах для определения $O_2$ в жидких средах.

К л ю ч е в ы е с л о в а: диоксид титана, церий, электровосстановление кислорода, каталитическая активность, фоточувствительность.

REFERENCES

1. ˇStengl V., Bakardjieva S., Murafa N. Preparation and photocatalytic activity of rare earth doped $TiO_2$ nanoparticles . *Mater.Chem. Phys.*2009. **114**: 217.
2. Stathatos E., Lianos P., Tsakiroglou C. Highly efficient nanocrystalline titania films made from organic/inorganic nanocomposite gels. *Micropor. Mesopor. Mat*. 2004. **75**: 255.
3. Matějová Lenka, Kočí Kamila, Reli Martin, Čapek Libor, Hospodková Alice, Peikertová Pavlína, Matěj Zdeněk, Obalová Lucie, Wach Anna, Kuśtrowski Piotr, Kotarba Andrzej. Preparation, characterization and photocatalytic properties of cerium doped $TiO_2$: On the effect of Ce loading on the photocatalytic reduction of carbon dioxide. *Appl. Catal., B*. 2014. **152–153**: 172.
4. Lin Jun, Yu Jimmy C. An investigation on photocatalytic activities of mixed $TiO_2$-rare earth oxides for the oxidation of acetone in ai**r.** *J.Photochem. Photobiology* A. 1998. **116(1)**: 63.
5. Fang J, Bi X, Si D, Jiang Z, Huang W. Spectroscopic studies of interfacial structures of $CeO_2$ –$TiO_2$ mixed oxides. *Appl Surf Sci*. 2007. **253**: 8952.
6. Matejova L., Vales V., Fajgar R., Matej, Z., Holy V; Solcova O. Reverse micelles directed synthesis of $TiO_2$-$CeO_2$ mixed oxides and investigation of their crystal structure and morphology. *J. Solid State Chem*. 2013. **198**: 485.
7. López T., Rojas F., Alexander-Katz R., Galindo F., Balankin A. S., Buljan A. Porosity, structural and fractal study of sol–gel $TiO_2$–$CeO_2$ mixed oxides. *J. Solid State Chem*. 2004. **177**: 1873.
8. Pavasupree S., Suzuki Y., Pivsa-Art S., Yoshikawa S. Preparation and characterization of mesoporous $TiO_2$–$CeO_2$ nanopowders respond to visible wavelength. *J. Solid State Chem*. 2005. **178**: 128.
9. Kolbasov G.Ya., Vorobets V. S., Korduban A. M., Shpak A. P., Medvedskii M. M., Kolbasova I. G., Linyucheva O. V. Electrodes Based on Nanodispersed Titanium and Tungsten Oxides for a Sensor of Dissolved Oxygen. Russ. J. Appl. Chem. 2006. **79(4)**: 596.


Надійшла 11.07.2019